Vol 17 No 8, August 2008
1674-1056/2008/17(08)/2867-07

Chinese Physics B

© 2008 Chin. Phys. Soc.
and IOP Publishing Ltd

Analytic equation of state for solids with multi-exponential potential based on analytic mean field potential approach and applied to the epsilon phase of solid oxygen*

Wang Li-Guo(王立国), Sun Jiu-Xun(孙久勋)†, and Yang Wei(杨 维)

Department of Applied Physics, University of Electronic Science and Technology, Chengdu 610054, *China*

(Received 5 September 2007; revised manuscript received 3 April 2008)

The thermodynamic properties of the ε phase of solid oxygen are studied by using the analytic mean field approach (AMFP). Analytic expressions for the Helmholtz free energy, internal energy and equation of state of solid oxygen have been derived based on the multi-exponential potential. The formulism for the case of double-exponential (DE) model is applied to the ε phase of solid oxygen. Its four potential parameters are determined through fitting the experimental compression data of the ε phase of solid oxygen. Numerical results of the pressure dependence of the volume calculated by using the AMFP are in good agreement with the original experimental data. This suggests that the AMFP is a useful approach to study the thermodynamic properties of the ε phase of solid oxygen. Furthermore, we predict the variation of the volume, lattice parameters and intermolecular distances with pressure, and some thermodynamic quantities versus volume, at several higher temperatures.

Keywords: analytic equation of state, analytic mean field approach, solid oxygen, ε phase
PACC: 0570C, 6410, 6430

1. Introduction

Solid oxygen has many unusual properties and thus attracts a great current interest from many scientific groups.[1−15] Solid oxygen shows successive phase transitions as the pressure and temperature change. The P–T structural phase diagram of oxygen described in Ref.[1] is shown in Fig.1. Since the first observation of dramatic colour changes above 10 GPa in experiments,[2] many studies on the properties of solid oxygen concerning the high-pressure phases have been reported.[3−13] Of all the properties of solid oxygen studied so far, the magnetic property has been an intriguing subject. Many experimental and theoretical studies on the magnetic property of the ε phase of solid oxygen have been reported.[9−13] Although there exist many reports on the magnetic property of the ε phase of solid oxygen, most of them are controversial. To date, the magnetic properties of the ε phase remain unclear since its structure problem has not been solved. Recently, Fujihisa *et al*[14] performed powder x-ray diffraction experiments and Rietveld analysis for the ε phase of solid oxygen. They proposed a structure that consisted of an O_8 cluster with 4 molecules in the ε phase of solid oxygen. The O_8 cluster structure model is consistent with both the results of optical experiments [8,10−12] and theoretical reports.[15] Thus, their work provided a new insight into the structure of the ε phase of solid oxygen.

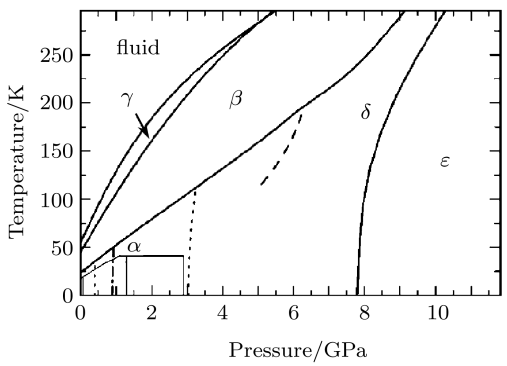


Fig.1. Phase diagram of solid oxygen at below room temperature and pressures up to 12 GPa, reproduced from Ref.[1].

*Project supported by the Joint Foundation of National Natural Science Foundation of China and China Academy of Engineering Physics (Grant No 10476007), by the Program for New Century Excellent Talents in University (Grant No NCET-05-0799), and the Program for Excellent Talents of University of Electronic Science and Technology (Grant No 23601008).
†Corresponding author. E-mail: sjx@uestc.edu.cn

We believe that theoretical study, especially on the thermodynamic properties, based on the new structure is very helpful for clarifying the magnetic structure of the ε phase. In recent years, many works on the equation of state (EOS) for solids have been reported.[16−39] For example, Xu proposed a revised Murnaghan equation; however, the revised equation is complex and not suitable for practical application.[16] Geng *et al* proposed a thermodynamic EOS appropriate to the investigation of shocked porous materials.[17−19] Sun *et al* proposed an analytic Debye–Grüneisen EOS for generalized Lennard-Jones solids and applied it to the research of the thermodynamic properties of solid xenon and krypton.[20−23] Although many theoretical works on the EOS have been reported, most of them do not take many important effects into account, such as the correlation effect at low temperatures and anharmonic effect at high temperatures. However, some studies[17−19,24,25] suggest that the anharmonic effect is important at high temperatures, and should be taken into account by using an appropriate approach.

Several years ago, Wang *et al*[26−29] proposed the analytic mean field potential (AMFP) approach, and applied it to many materials. Bhatt *et al*[30,31] further applied the AMFP to lead and alkali metals, and concluded that in comparison with other theoretical models the AMFP is computationally simple, physically transparent and reliable for the study of thermodynamic properties at high pressures and high temperatures. Zhang *et al*[32] combined first-principles treatment for electronic contribution and the AMFP for the vibrational contribution of the lattice ions to calculate thermodynamic properties of shock-compressed BeO. The calculated Hugoniot shows good agreement with the experimental data.

Sun *et al* have proven that the AMFP is an analytic approximation of the free volume theory (FVT).[33] The AMFP has been applied to solid C_{60} by using the Girifalco potential[34] also by Sun *et al*,[35] the numerical results of which are in good agreement with the molecular dynamics (MD) simulations[36,37] and superior to the CUST of Zubov *et al*.[38,39] This verifies that the AMFP is a convenient approach to consider the anharmonic effects at high temperatures. Thus, in this paper, we present the results of thermodynamic properties of the ε phase in solid oxygen studied by using the AMFP.

It is very important to adopt an appropriate potential function for the application of AMFP. Generally, the Lennard-Jones, exponential-6, Girifalco and double exponential (DE) potentials (or generalized Morse potential) are used. However, the computer simulations have shown that the Lennard-Jones and original Girifalco potentials are not able to describe the solid-state behaviour even at moderate high pressures.[36,37] As for the exponential potential, it is appropriate to describe the properties of the majority materials at high pressures. Considering these aspects, we use the double exponential (DE) potential (or generalized Morse potential) in the present work.

The rest of this paper is organized as follows. In Section 2 we derive the analytic EOS based on the AMFP approach. In Section 3, the parameters of the DE potential are determined by fitting the experimental data of the pressure dependence of the molar volume of the ε phase in solid oxygen, and the numerical results of thermodynamic properties are calculated and compared with the experimental data. Finally, the conclusion is given in Section 4.

2. Analytic equation of state

The multi-exponential potential is expressed as

$$\varepsilon(s) = \varepsilon_0 \cdot \sum_{j=1}^{m} C_j \exp[\lambda_j(1 - r/r_0)], \tag{1}$$

where r_0 is the equilibrium distance, ε_0 is the well depth. For the DE potential, we have $m = 2$ and

$$\begin{aligned} C_1 &= \lambda_2/(\lambda_1 - \lambda_2), \\ C_2 &= -\lambda_1/(\lambda_1 - \lambda_2). \end{aligned} \tag{2}$$

The two parameters λ_1 and λ_2 describe the decrease of potential as the distance increases.

In terms of the FVT, the free energy can be expressed as[20−29,34−39]

$$\frac{F}{NkT} = -\frac{3}{2}\ln\left(2\pi\mu kT/h^2\right) + \frac{E(a)}{kT} - \ln v_{\mathrm{f}}, \tag{3}$$

where μ is the mass of solid oxygen molecules, $E(a)$ is the cohesive energy of a molecule as the lattice is static, v_{f} is the free volume.

$$E(a) \equiv E(y) = \varepsilon_0 \cdot \sum_{j=1}^{m} C_j \exp[\lambda_j(1 - y)], \tag{4}$$

where a is the nearest-neighbour distance.

$$v_{\mathrm{f}} = 4\pi \int_0^{r_m} \exp[-g(r, V)/kT] r^2 \mathrm{d}r. \tag{5}$$

Here $g(r, V)$ is the potential energy of a molecule as it goes from the centre to a distance r. In terms of

the AMFP approach,[26−29] $g(r,V)$ can be expressed as the static energy $E(a)$ of a molecule

$$g(r,V) = \frac{1}{2}\left[\left(1+\frac{r}{a}\right)E(a+r) + \left(1-\frac{r}{a}\right)E(a-r) - 2E(a)\right]. \quad (6)$$

Let r_m be the largest displacement, its value can be approximately taken as the Wigner–Seitz radius, $r_m = \left(3a^3/4\pi\gamma\right)^{1/3} \approx a/2$, with a being the nearest-neighbour distance, and γ the structure constant. For fcc structure, we have $\gamma = \sqrt{2}$, and $r_m \approx a/1.81$. For bcc structure, we have $\gamma = 3\sqrt{3}/4$, and $r_m \approx a/1.76$. However, our calculations show that the results are not sensitive to the values of γ or r_m, thus we approximately take $r_m \approx a/2$ for convenience.

The volume of solid oxygen molecules is $V = Na^3/\gamma$. For simplicity, we introduce the dimensionless reduced free volume $\bar{v}_\mathrm{f}$, reduced volume y, and reduced radial coordinate x as follows:

$$v_\mathrm{f} = 4\pi a^3 \bar{v}_\mathrm{f} = 4\pi\gamma V \bar{v}_\mathrm{f}, \quad (7)$$

$$y = a/r_0 = (V/V_0)^{1/3}, \quad V_0 = N\left(r_0\right)^3/\gamma. \quad (8)$$

$$x = r/a, \quad x_m = \frac{r_m}{a} \approx \frac{1}{2}. \quad (9)$$

The reduced free volume $\bar{v}_\mathrm{f}$ and its derivatives with respect to temperature and reduced volume can be expressed as

$$\bar{v}_\mathrm{f} = \int_0^{x_m} \exp\left[-g\left(x,y\right)/kT\right]x^2\mathrm{d}x, \quad (10)$$

$$\bar{v}_{\mathrm{f}a} = T\frac{\partial}{\partial T}\bar{v}_\mathrm{f} = \frac{1}{kT}\int_0^{x_m} \exp\left[-g\left(x,y\right)/kT\right] \cdot g\left(x,y\right)x^2\mathrm{d}x, \quad (11)$$

$$\bar{v}_{\mathrm{f}b} = -\frac{\partial}{\partial y}\bar{v}_\mathrm{f} = \frac{1}{kT}\int_0^{x_m} \exp\left[-g\left(x,y\right)/kT\right] \cdot \frac{\partial}{\partial y}g\left(x,y\right)x^2\mathrm{d}x, \quad (12)$$

$$\bar{v}_{\mathrm{f}c} = \frac{1}{2}\left(\frac{x_m}{y}\right)^2 \exp\left[-g\left(x_m,y\right)/kT\right] \approx 0. \quad (13)$$

Here $g\left(x,y\right) \equiv g\left(r,V\right)$, and combining Eqs.(4) and (7), we have

$$g(x,y) \equiv g(r,V) \approx \frac{1}{2}[(1+x)E(y+yx) + (1-x)E(y-yx) - 2E(y)], \quad (14)$$

$$\frac{\partial}{\partial y}g(x,y) \approx \frac{1}{2}[(1+x)^2E'(y+yx) + (1-x)^2E'(y-yx) - 2E'(y)], \quad (15)$$

$$E'(y) = -\varepsilon_0 \cdot \sum_{j=1}^{m} \lambda_j C_j \exp[\lambda_j(1-y)]. \quad (16)$$

The compressibility factor and internal energy can be derived as

$$Z = \frac{PV}{NkT} = -\frac{y}{3}\frac{\partial}{\partial y}\frac{F}{NkT} = \frac{P_\mathrm{c}V}{NkT} + \frac{P_\mathrm{f}V}{NkT}, \quad (17)$$

$$\frac{P_\mathrm{c}V}{NkT} = -\frac{y}{3kT}\frac{\partial}{\partial y}E\left(y\right) = -\frac{y}{3kT}E'\left(y\right), \quad (18)$$

$$\frac{P_\mathrm{f}V}{NkT} = 1 + \frac{y}{3\bar{v}_\mathrm{f}}\frac{\partial}{\partial y}\bar{v}_\mathrm{f} = 1 - \frac{y}{3\bar{v}_\mathrm{f}}\left(\bar{v}_{\mathrm{f}b} - \bar{v}_{\mathrm{f}c}\right) \approx 1 - \frac{y\bar{v}_{\mathrm{f}b}}{3\bar{v}_\mathrm{f}}, \quad (19)$$

$$\frac{U}{NkT} = -T\frac{\partial}{\partial T}\frac{F}{NkT} = \frac{3}{2} + \frac{E\left(y\right)}{kT} + \frac{T}{\bar{v}_\mathrm{f}}\frac{\partial\bar{v}_\mathrm{f}}{\partial T} = \frac{3}{2} + \frac{E\left(y\right)}{kT} + \frac{\bar{v}_{\mathrm{f}a}}{\bar{v}_\mathrm{f}}, \quad (20)$$

where P_c is the cold pressure, P_f is the thermal pressure deduced from the free volume.

By using the above equations, all other thermodynamic quantities can be analytically derived, and the derivations are straightforward. However, the expressions for thermal expansivity, compressibility coefficient and isochoric heat capacity are redundant, we would calculate these quantities by using numerical differentiation instead of the analytic expressions. The compressibility factor can be regarded as a function of variables y and T, $Z = Z\left(y,T\right)$. In terms of this function, the formulas for thermal expansivity, compressibility coefficient and isochoric heat capacity can be reduced to the following form:

$$\alpha = \frac{1}{V}\left(\frac{\partial V}{\partial T}\right)_P = \frac{3}{y}\left(\frac{\partial y}{\partial T}\right)_P = \left[\frac{Z}{T} + \left(\frac{\partial Z}{\partial T}\right)_y\right]\left[Z - \left(\frac{y}{3}\right)\left(\frac{\partial Z}{\partial y}\right)_T\right]^{-1}, \quad (21)$$

$$\beta = -\frac{1}{V}\left(\frac{\partial V}{\partial P}\right)_T = -\frac{3}{y}\left(\frac{\partial y}{\partial P}\right)_T = \left(\frac{V_d y^3}{NkT}\right)\left[Z - \left(\frac{y}{3}\right)\left(\frac{\partial Z}{\partial y}\right)_T\right]^{-1}, \quad (22)$$

$$\frac{C_V}{Nk} = \frac{1}{Nk}\left(\frac{\partial U}{\partial T}\right)_V = \frac{U}{NkT} + T\frac{\partial}{\partial T}\left(\frac{U}{NkT}\right)_y. \quad (23)$$

In our calculations, it is found that following steps for the numerical differentiations in Eqs.(21)–(23) can reach stable numerical results, $\Delta T = 0.00001 \times T$ and $\Delta y = 0.00001 \times y$.

3. Results and discussion

In this section, we apply the above formulism to the ε phase of solid oxygen. We determine the parameters for the DE potential in Eq.(4) by fitting the experimental data of the pressure dependence of the molar volume at 300 K.[14] The average error for the pressure of the ε phase of solid oxygen is merely 0.94%. And the determined values of the parameters are as follows:

$$\lambda_1 = 10.7, \quad \lambda_2 = 5.7,$$
$$r_0 = 0.3445\,\text{nm}, \quad \varepsilon_0 = 4855\,\text{K}. \tag{24}$$

Substituting Eq.(24) into Eq.(4) yields the following cohesive energy of a molecule:

$$E(a) = 4855\left[1.14\text{e}^{10.7(1-a/0.3445)} - 2.14\text{e}^{5.7(1-a/0.3445)}\right]. \tag{25}$$

The unit of energy in Eq.(25) is K. In terms of Eq.(25), we plot $E(a)$ versus the nearest-neighbour distance a in Fig.2. Furthermore, we calculate the numerical results of the pressure dependence of the volume by using the AMFP, and compare our results with the original experimental data in Fig.3. It is shown that our results are in fairly good agreement with the original experimental data both at low and high pressures. This suggests that the AMFP is a useful approach to study the thermodynamic properties of the ε phase of solid oxygen. At the same time, we predict the pressure dependence of the volume at several higher temperatures (T = 800, 1400, and 2000 K), and also plot the results in Fig.3. The figure shows that the compression curves get soft as the temperature increases.

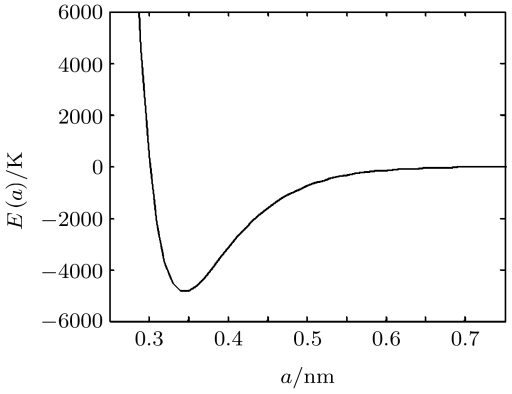


Fig.2. The cohesive energy of a molecule, $E(a)$, as a function of the nearest-neighbour distance a for the ε phase of solid oxygen (ε-solid O_2).

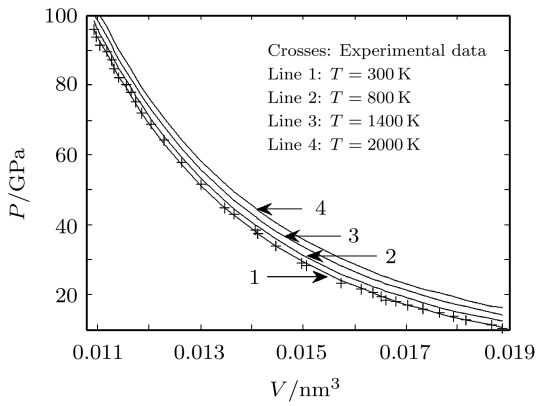


Fig.3. Comparison of the isothermals of the ε- solid O_2 calculated in this work by using the AMFP at 300 K (line 1) with the experimental data by Fujihisa *et al* in Ref.[14] at 300 K (cross marks). Furthermore, the comparison of isothermals of the ε-solid O_2 calculated in this work by using the AMFP at 300 K (line 1) with the results predicted in this work by using the AMFP at 800 K (line 2), 1400 K (line 3) and 2000 K (line 4).

Considering that the study on the lattice parameters and the intermolecular distances is very important for determining the crystal structure of the ε phase of solid oxygen, we predict the pressure dependence of them at several higher temperatures by using the AMFP (T = 800, 1400, and 2000 K). In terms of AMFP, we treat the lattice parameters and the intermolecular distances as functions of reduced volume y, and treat the reduced volume y as a function of pressure P and temperature T. If the compression of the ε phase of solid oxygen is isotropic, the variations of the lattice parameters with pressure should be identical, i.e., the variations should have the same function form. The relationship can be expressed as follows:

$$b_i = b_i(P,T) = b_{i0}\,y(P,T), \quad (i = 1,2,3); \tag{26}$$
$$d_i = d_i(P,T) = d_{i0}\,y(P,T), \quad (i = 1,2). \tag{27}$$

In Eq.(26), the subscripts i = 1, 2, 3 represent the lattice parameters a, b and c in Ref.[14], respectively. And in Eq.(27), the subscripts i = 1, 2 represent the intermolecular distances d_1 and d_2, respectively.[14] However, we find that Eqs.(26) and (27) cannot describe the experimental data of lattice parameters versus pressure satisfactorily.

In order to determine the accurate expressions $b_i(P,T)$ and $d_i(P,T)$, we adopt following procedure instead of Eqs.(26) and (27). Firstly, we calculate the values of reduced volume y and pressure P by using the AMFP at T = 300 K. Secondly, we determine the $y(P,T)$ by fitting it with the data of y and P. Finally, we derive the accurate expressions of $b_i(P,T)$

and $d_i\,(P,T)$ by fitting the experimental data of the pressure dependence of the lattice parameters and the intermolecular distances at $T = 300\,\mathrm{K}$[14] and $y\,(P,T)$. The expressions are as follows:

$$\begin{aligned} y = & -5.0 \times (P/100)^7 + 19.8 \times (P/100)^6 \\ & -34.5 \times (P/100)^5 + 32.2 \times (P/100)^4 \\ & -17.5 \times (P/100)^3 + 5.82 \times (P/100)^2 \\ & -1.31 \times (P/100) + 0.962, \end{aligned} \tag{28}$$

$$b_1 = 5.65 + 4.4y^{4.38}, \tag{29}$$

$$b_2 = 6.78y^{1.27}, \tag{30}$$

$$b_3 = 4.2y^{0.81}, \tag{31}$$

$$d_1 = 1.57 + 1.21y^{3.9}, \tag{32}$$

$$d_2 = 0.68 + 2.51y^{1.68}. \tag{33}$$

In Eqs.(28)–(32), the unit of pressure is GPa, and the unit of length is nm. From Eqs.(29)–(31), we can see that the form of Eq.(29) is different from Eqs.(30) and (31). The result is not consistent with theoretical prediction in Eq.(26). This implies that the compression of the ε phase of solid oxygen may be anisotropic. Moreover, we know that the dependences of the lattice parameters b_1, b_2 and b_3 on the pressure are all decreasing monotonically, and the volume of unit cell is equal to $b_1 b_2 b_3 \cdot \sin\beta$. Thus the sum of exponents contained in Eqs.(29)–(31) should be approximately equal to 3. Whereas the results in Eqs.(29)–(31) also are not consistent with the theoretical prediction. We postulate that the reason may be that the experimental data of lattice parameters and molar volume in Ref.[14] have been measured in separate experiments, and thus are not self-consistent.

In order to predict the pressure dependence of the lattice parameters and the intermolecular distances at several higher temperatures, we calculate the reduced volume y and the pressure P at several higher temperatures by using the AMFP. Then we apply these data to Eqs.(28)–(33). In Figs.4–8, we plot the predicted results of pressure dependence of the lattice parameters and the intermolecular distances at several higher temperatures. From Figs.4–8, we can see that the higher the temperature, the greater the slope of the curve. This means that the temperature has a significant effect on the lattice parameters and the intermolecular distances at relative low pressures.

In Figs.9–11, we present the results of thermodynamic properties of the ε phase of solid oxygen calculated by using the AMFP. Figure 9 illustrates the variation of isochoric heat capacity C_V, thermal expansivity α and bulk modulus B_T with pressure for several temperatures. The figure shows that C_V increases slowly with increasing pressure and decreases with increasing temperature. Whereas α is a decreasing function of pressure, and an increasing function of temperature. The decrease is fast at low pressures,

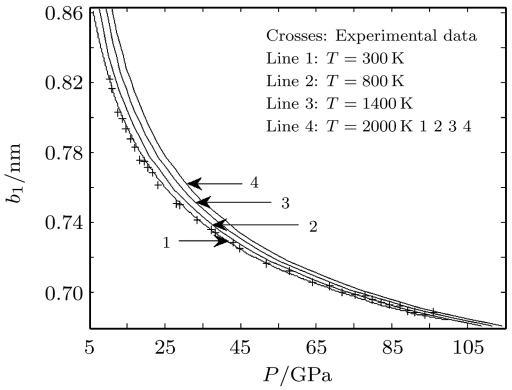


Fig.4. Pressure dependence of the structural parameter b_1 of the ε- solid O_2, for the lattice parameter a. The cross marks are the original experimental data by Fujihisa *et al* in Ref.[14]. Line 1 is the fitting curve by using the AMFP at 300 K. The other three lines are our predicted results for 800 K (line 2), 1400 K (line 3), and 2000 K (line 4).

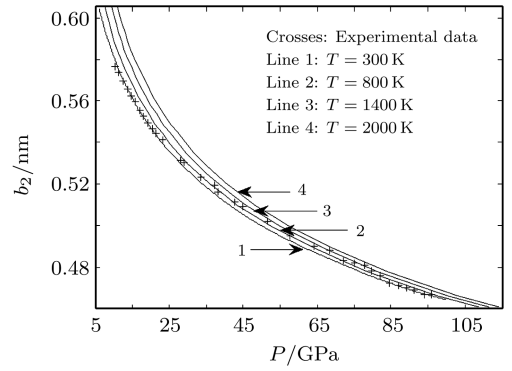


Fig.5. Same as Fig.4, but for the lattice parameter b_2.

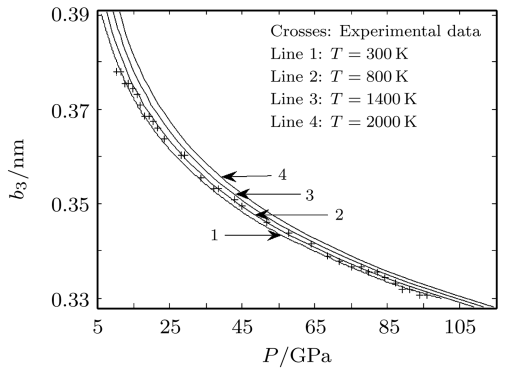


Fig.6. Same as Fig.4, but for the lattice parameter b_3.

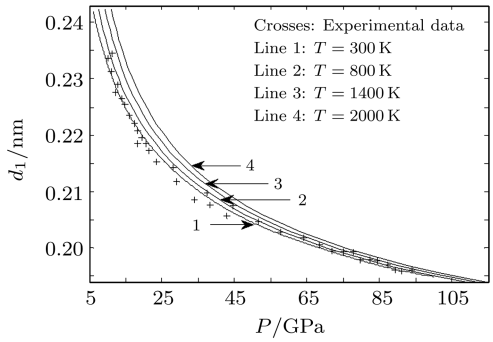


Fig.7. Pressure dependence of the structural parameters of ε-solid O_2, for the intermolecular distance d_1. The cross marks are the original experimental data by Fujihisa *et al* in Ref.[14]. Line 1 is the fitting curve by using the AMFP at 300 K. The other three lines are our predicted results for 800 K (line 2), 1400 K (line 3), 2000 K (line 4).

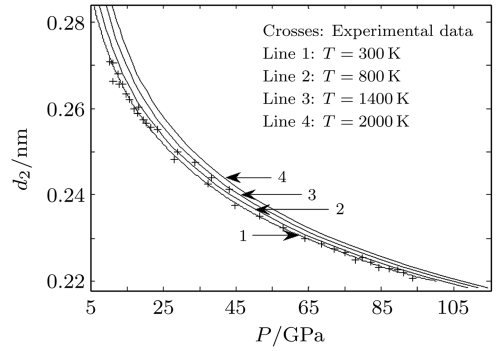


Fig.8. Same as Fig.7, but for the intermolecular distance d_2.

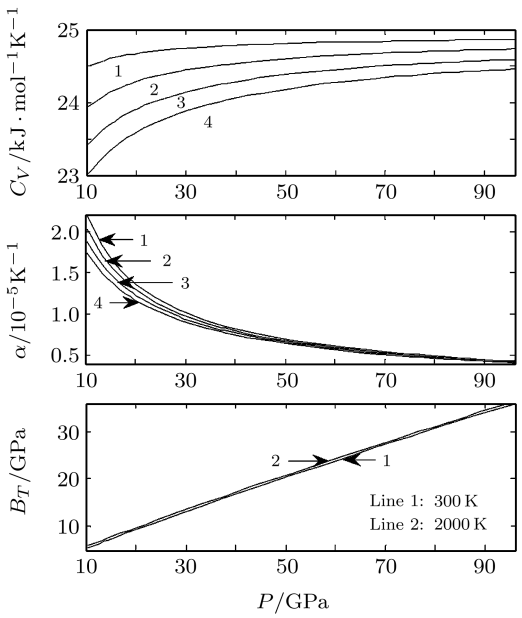


Fig.9. Variations of the heat capacity C_V and the thermal expansion coefficient α with pressure calculated in this work by using the AMFP at 300 K (line 1), 800 K (line 2), 1400 K (line 3), and 2000 K (line 4). And the variation of the bulk modulus B_T with pressure, calculated at 300 K (line 1) and 2000 K (line 2). The heat capacity is in kJ·mol^{-1}K^{-1}, linear thermal expansion coefficient in 10^{-5} K^{-1}, and the bulk modulus in GPa.

and it slows down as the pressure increases. B_T is a linearly increasing function of pressure. The change of slope of B_T versus pressure is rather small. This means that the solid oxygen is easy to be compressed. The difference between the two lines of B_T at 300 and 2000 K is invisible in Fig.9, and this implies that B_T is a weak increasing function of temperature. In Figs.10 and 11, we plot the variations of free energy and internal energy versus the volume at four temperatures. The two figures show that both the free energy and the internal energy are decreasing function of volume, and the two quantities have the same variation tendency as the volume increases for different temperatures.

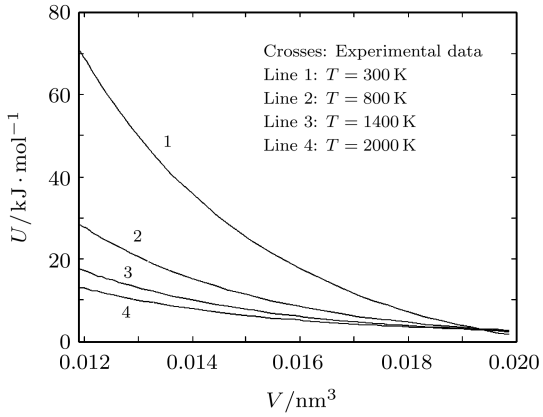


Fig.10. Internal energy U as a function of volume calculated for four temperatures by using the AMFP. The four different lines represent results for 300 K (line 1), 800 K (line 2), 1400 K (line 3), and 2000 K (line 4).

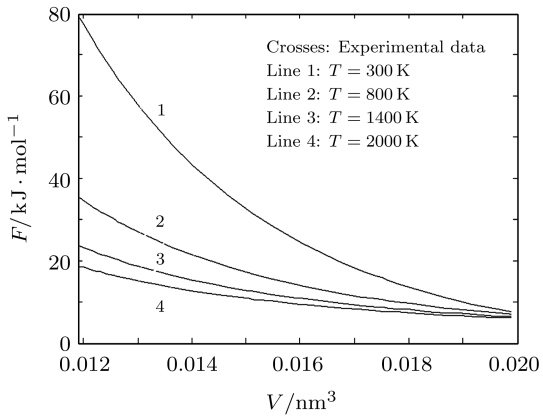


Fig.11. Free energy F as a function of volume calculated for four temperatures by using the AMFP. The four different lines represent results for 300 K (line 1), 800 K (line 2), 1400 K (line 3), 2000 K (line 4), respectively.

4. Conclusion

In summary, the AMFP approach has been applied to the ε phase of solid oxygen. The analytic expressions for the Helmholtz free energy, internal en-

ergy and EOS have been derived. By fitting the experimental data with the pressure dependence of the molar volume at 300 K, we determine the parameters for the DE potential. Furthermore, we calculate the pressure dependence of the volume by using the AMFP. The results obtained are in good agreement with the previous experimental data. This suggests that the AMFP is an appropriate approach to study the thermodynamic properties of solid oxygen. By means of formulism derived in this paper based on the AMFP, we also calculate some thermodynamic quantities of the ε phase of solid oxygen and predict the variation tendency of some thermodynamic quantities with volume, and the dependence of the lattice parameters and the intermolecular distances on pressure for several higher temperatures.

References

[1] Kreutz J, Medvedev S A and Jodl H J 2005 *Phys. Rev.* B **72** 214115

[2] Nicol M, Hirsch K R and Holzapfel W B 1979 *Chem. Phys. Lett.* **68** 49

[3] Akahama Y, Kawamura H, Hausermann D, Hanfland M and Shimomura O 1995 *Phys. Rev. Lett.* **74** 4690

[4] Weck G, Loubeyre P and LeToullec R 2002 *Phys. Rev. Lett.* **88** 035504

[5] Desgreniers S, Vohra Y K and Ruoff A L 1990 *J. Phys. Chem.* 94 1117

[6] Shimizu K, Suhara K, Ikumo M, Eremets M I and Amaya K 1998 *Nature* (London) **393** 767

[7] Goncharov A F, Gregoryanz E, Hemley R J and Mao H K 2003 *Phys. Rev.* B **68** 100102(R)

[8] Agnew S F, Swanson B I and Jones L H 1987 *J. Chem. Phys.* **86** 5239

[9] Gebauer R, Serra S, Chiarotti G L, Scandolo S, Baroni S and Tosatti E 2000 *Phys. Rev.* B **61** 6145

[10] Gorelli F A, Ulivi L, Santoro M and Bini R 1999 *Phys. Rev. Lett.* **83** 4093

[11] Gorelli F A, Ulivi L, Santoro M and Bini R 2001 *Phys. Rev.* B **63** 104110

[12] Santoro M, Gorelli F A, Ulivi L, Bini R and Jodl H J 2001 *Phys. Rev.* B **64** 064428

[13] Goncharenko I N 2005 *Phys. Rev. Lett.* **94** 205701

[14] Fujihisa H, Akahama Y, Kawamura H, Ohishi Y, Shimomura O, Yamawaki H, Sakashita M, Gotoh Y, Takeya S and Honda K 2006 *Phys. Rev. Lett.* **97** 085503

[15] Neaton J B and Ashcroft N W 2002 *Phys. Rev. Lett.* **88** 205503

[16] Xu J A 1976 *Acta Phys. Sin.* **25** 324 (in Chinese)

[17] Geng H Y, Tan H and Wu Q 2001 *Chin. Phys.* **10** 433

[18] Geng H Y, Tan H and Wu Q 2002 *Chin. Phys. Lett.* **19** 531

[19] Geng H Y, Wu Q, Tan H, Cai L C and Jing F Q 2002 *Chin. Phys.* **11** 1188

[20] Sun J X, Cai L C, Wu Q and Jing F Q 2000 *Chin. Phys.* **9** 927

[21] Sun J X, Wu Q, Cai L C and Jing F Q 2002 *Chin. Phys.* **9** 1009

[22] Sun J X, Wu Q, Cai L C and Jing F Q 2003 *Chin. Phys.* **12** 632

[23] Sun J X, Yang H C, Wu Q and Cai L C 2002 *J. Phys. Chem. Solids* **63** 113

[24] Shukla R C and Cowley E R 1985 *Phys. Rev.* B **31** 374

[25] Lacks D J and Shukla R C 1996 *Phys. Rev.* B **54** 3266

[26] Wang Y, Chen D and Zhang X 2000 *Phys. Rev. Lett.* **84** 3220

[27] Wang Y 2000 *Phys. Rev.* B **62** 196

[28] Wang Y 2001*Phys. Rev.* B **63** 245108

[29] Wang Y, Ahuja R and Johansson B 2001 *Phys. Rev.* B **65** 014104

[30] Bhatt N K, Jani A R, Vyas P R and Gohel V B 2001 *Physica* B **65** 014104

[31] Bhatt N K, Vyas P R, Jani A R and Gohel V B 2005 *J. Phys. Chem. Solids* **66** 797

[32] Zhang Q L, Zhang P, Song H F and Liu H F 2008 *Chin. Phys* **17** 1341

[33] Sun J X, Cai L C, Wu Q and Jing F Q 2005 *Phys. Rev.* B **71** 024107

[34] Girifalco L A 1992 *J. Phys. Chem.* **96** 858

[35] Sun J X 2006 *Physica* B **34** 381

[36] Abramo M C and Caccamo C 1996 *J. Phys. Chem. Solids* **57** 1751

[37] Abramo M C, Caccamo C, Costa D, Pellicane G and Ruberto R 2004 *Phys. Rev.* E **69** 031112

[38] Zubov V I, Tretiakov N P, Sanchez J F and Caparica A A 1996 *Phys. Rev.* B **53** 12080

[39] Zubov V I, Sanchez-Ortiz J F, Tretiakov N P and Zubov I V 1997 *Phys. Rev.* B **55** 6747